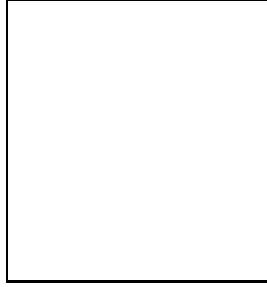


LIGHT MESONS FROM CHARM MESON DECAYS IN FNAL E791

B. T. MEADOWS ^a
Department of Physics
University of Cincinnati ^b
Cincinnati, OH, USA



An analysis of the Dalitz plots for the decays $D^+ \rightarrow K^- \pi^+ \pi^+$ and $D^+ \rightarrow \pi^- \pi^+ \pi^+$ indicates that structure with significant phase variation is required in the s -wave $K^- \pi^+$ and $\pi^- \pi^+$ systems in the region below 1 GeV/c² effective mass. A constant, non resonant “contact” term, together with a simple s -wave Breit Wigner amplitude with $M_o = 797 \pm 19 \pm 43$, $\Gamma_o = 175 \pm 12 \pm 12$ MeV/c² for the $K^- \pi^+$ system and $M_o = 478^{+24}_{-23} \pm 17$, $\Gamma_o = 324^{+42}_{-40} \pm 21$ MeV/c² for the $\pi^- \pi^+$ system provide good fits to the data in this region.

1 Introduction

Decays of D mesons to three pseudo scalar mesons can produce intermediate, two meson systems with natural parity. Kinematics and angular momentum barrier factors generally favour scalar ($J^P = 0^+$) over vector 1^- or tensor 2^+ systems. Analysis of these decays can therefore provide new information on the poorly understood scalar meson system.

In most instances, D decays appear to proceed through quasi two body channels. In the cases of D^+ decays ^c to $\pi^- \pi^+ \pi^+$ and to $K^- \pi^+ \pi^+$ however, intermediate states found in the Particle Data Group listings ¹ (PDG) have been found to contribute only partially to the decays, with three body modes apparently dominant ^{2,3}. We report here on analyses ^{4,5} of these decays using the largest samples so far examined.

^aRepresenting the E791 collaboration.

^bSupported by NSF grant 9901568.

^cExcept where indicated otherwise, charge conjugate systems are implied in this paper.

2 Fermilab Experiment E791

In this experiment 6×10^{10} charm enhanced interactions between 500 GeV/c π^- mesons and thin foil targets (four C , one Pt) are recorded⁷. Foils are spaced so that decays of D mesons produced in them occur predominantly between them. Silicon strip detectors measure D decay lengths (mean ~ 5 mm) with a typical precision of 350 μm . Charged particle momenta are measured with two dipole magnets and drift chambers and two threshold gas Cherenkov detectors provide $K/\pi/p$ separation in the 6-60 GeV/c momentum range.

Events with one negative and two positive charged tracks making a good vertex, well separated from any foil and from the primary interaction point, are selected for further analysis. The resultant momentum is required to point back to within 40 μm of the primary vertex. For the $K^-\pi^+\pi^+$ sample the K^- is required to have momentum $6 \text{ GeV/c} < |\vec{p}_K| < 40 \text{ GeV/c}$ and to be identified by the Cherenkov detectors. Other cuts are also made to reduce contamination from tracks that are really associated with the primary vertex. With these selection criteria, the major sources of background are mostly misidentified (or incomplete) charm decays, with a small, “combinatorial” contribution from false secondary vertices. Yields of 15,090 $K^-\pi^+\pi^+$ (6% background) and 1,686 $\pi^-\pi^+\pi^+$ (28% background) remain in the signal regions.

3 Isobar Analysis of D Decay to Three Pseudo-Scalars

Decays of D mesons to three pseudo scalars i, j, k can be described approximately as a sum of isobar amplitudes, each corresponding to a quasi two body decay $D \rightarrow R(\rightarrow i j) k$. Each amplitude must satisfy Lorentz invariance and conserve total spin and has the form

$$\mathcal{A}_R(s_{ij}, s_{ik}) = F_D(q, r_D) F_R(p, r_R) \times BW_R(s_{ij}) \times (-2)^J |\vec{p}|^J |\vec{q}|^J P_J(\cos \theta)$$

where \vec{p}, \vec{q} are momenta of i and k respectively in the (ij) rest frame and $\cos \theta = \hat{p} \cdot \hat{q}$. Form factors F_D (F_R) for D (R) are parametrized in terms of effective radii R_D (R_R). A Breit Wigner propagator $BW_R = [s_R - s_{ij} - i\sqrt{s_R} \Gamma(s_{ij})]^{-1}$ describes the resonance R with spin J , mass $\sqrt{s_R}$. Suffix R denotes a quantity evaluated at $s_{ij} = s_R$.

A decay is kinematically specified by coordinates (s_{ij}, s_{ik}) on a Dalitz plot and by the three body mass M_{ijk} whose distribution about the D mass m_D due to resolution is $G(M_{ijk})$, determined from the data. The signal distribution of decays is

$$\mathcal{P}_S(s_{ij}, s_{ik}, M_{ijk}) = G(M_{ijk}) \times \left| a_{NR} e^{i\delta_{NR}} + \sum_R a_R e^{i\delta_R} \mathcal{A}_R(s_{ij}, s_{ik}) \right|^2$$

in which three body decays (NR) are described by a constant, “contact” amplitude $a_{NR} e^{i\delta_{NR}}$.

The distribution $\mathcal{P}_B(s_{ij}, s_{ik}, M_{ijk})$ of backgrounds is modelled using events from side bands in M_{ijk} for combinatorial, and from MC simulations for broken charm sources. The efficiency $\epsilon(s_{ij}, s_{ik})$ for observing decays is determined from MC simulations.

Complex coefficients $a e^{i\delta}$ and resonance parameters are determined from fits to a linear combination of $\epsilon \mathcal{P}_S$ and \mathcal{P}_B in the correct proportions. The fraction of D decay to an isobar R is $f_R = G(M_{ijk}) \int |\mathcal{A}_R|^2 ds_{ij} ds_{ik} / \int \mathcal{P}_S ds_{ij} ds_{ik}$ evaluated at $M_{ijk} = m_D$.

4 The $K^-\pi^+\pi^+$ Channel.

The Dalitz plot in figure 1(a) shows clear bands in the $\overline{K}_1(890)$ regions with an asymmetric structure indicative of interference with a significant, underlying s -wave. An accumulation of events near 2 $(\text{GeV}/c^2)^2$ indicates contributions from $\overline{K}_0(1430)$ or $\overline{K}_2(1430)$. A fit is made including isobar amplitudes for these resonances and the $\overline{K}_1(1688)$, each with mass and width

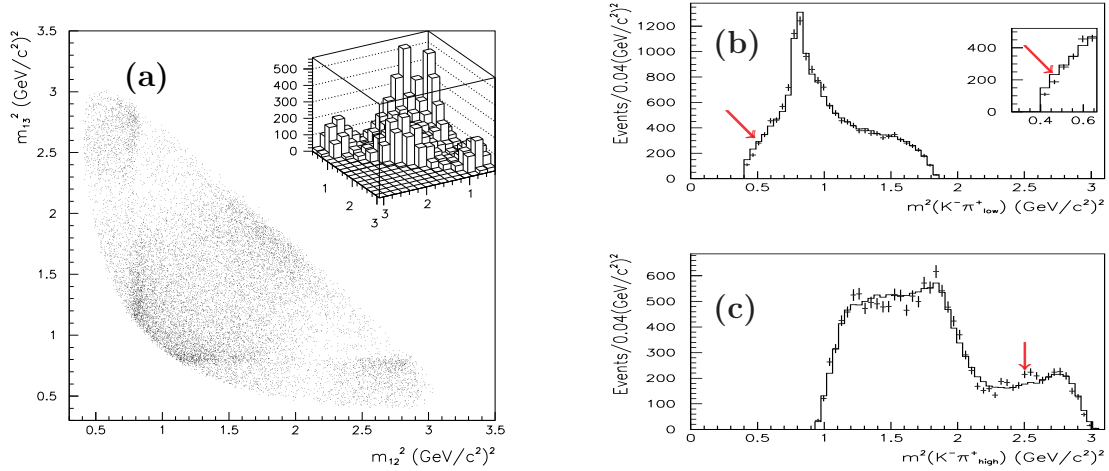


Figure 1: (a) Dalitz plot for $D^+ \rightarrow K^-\pi^+\pi^+$ decays. Projections for (b) smaller and (c) larger $K\pi$ effective mass for data (crosses) and fit (line) to model I described in the text. Arrows indicate regions where the fit is worst.

fixed at their PDG values. Results are shown in table 1 (model I) and compared with the $K^-\pi^+$ mass projections in figures 1(b) and (c). As in previous analyses^{2,3} using this model, a large NR component is required ($\sim 90\%$) and the sum of all contributions is $\sim 140\%$ indicating much destructive interference. The fit is poor with a χ^2 , found by comparing predictions of model I

Table 1: Resonant fractions f for $D^+ \rightarrow K^-\pi^+\pi^+$, and $\pi^-\pi^+\pi^+$. Models I-IV are described in the text.

$D^+ \rightarrow$	$K^-\pi^+\pi^+$	$\kappa\pi$	$K_1(890)\pi$	$K_0(1430)\pi$	$K_2(1430)\pi$	$K_1(1688)\pi$
I	90.0 ± 2.6	-	13.8 ± 0.5	30.6 ± 1.6	0.4 ± 0.1	3.2 ± 0.3
II	13.0 ± 5.8 ± 4.4	47.8 ± 12.1 ± 5.3	12.3 ± 1.0 ± 0.9	12.5 ± 1.4 ± 0.5	0.5 ± 0.1 ± 0.2	2.5 ± 0.7 ± 0.3
$D^+ \rightarrow$	$\pi^-\pi^+\pi^+$	$\sigma\pi$	$\rho(770)\pi$	$f_0(980)\pi$	$f_2(1270)\pi$	$\rho(1450)\pi$
III	38.6 ± 1.4	-	20.8 ± 2.3	7.4 ± 4.3	6.3 ± 3.3	22.6 ± 2.1
IV	7.8 ± 6.0 ± 2.7	46.3 ± 9.0 ± 2.1	33.6 ± 3.2 ± 2.2	6.2 ± 1.3 ± 0.4	19.4 ± 2.5 ± 0.4	0.7 ± 0.7 ± 0.3

with data in equal square bins in the Dalitz plot, of 167 for 63 degrees of freedom ν . Major discrepancies are at low $K^-\pi^+$ masses, and the corresponding high mass reflection, and can be seen in earlier data for both this channel³ and for $D^0 \rightarrow K^-\pi^+\pi^0$ ⁸. However the large E791 sample underlines their significance, and demands that a better model be found.

First, the radii R_D , R_R and the mass and width of $K_0(1430)$ are allowed to float⁹. This produces little improvement. Next, a further scalar amplitude “ κ ” having a Breit Wigner form similar to $K_0(1430)$ is added (model II in Table 1). This does provide an excellent description of the data with $\chi^2/\nu = 46/63$. The κ mode is dominant while the NR component is consistent with zero. The sum of fractions is $\sim 86\%$. The κ mass and width, determined from the fit, are $M_\kappa = 797 \pm 19 \pm 43$ and $\Gamma_\kappa = 175 \pm 12 \pm 12$ MeV/c². In this model, however, the $K_0(1430)$ mass and width are found to be $1459 \pm 7 \pm 12$ MeV/c² and $175 \pm 12 \pm 12$ MeV/c² respectively, differing somewhat from the values from LASS⁹.

The s -wave BW form used for the κ in model II appears to be important. Variations in this, or in form factors for κ and NR terms, are found to affect principally the amounts of κ and NR, but to have relatively small effects on κ mass and width parameters. Replacing the complex BW in model II by its absolute magnitude (a “ κ ” mass enhancement, but no phase variation) results in unphysically large κ and NR fractions. A vector form for κ converges with mass ~ 1100 MeV/c² and negligible fraction. A tensor κ fit fails to converge.

5 $D^+ \rightarrow \pi^- \pi^+ \pi^+$ Decays.

Figure 2(a) is the Dalitz plot for these decays⁴. Table 1 shows results for model III in which only resonances from the PDG are included. The fit is poor ($\chi^2/\nu = 1.5$), especially in the low mass $\pi^- \pi^+$ system as seen in figure 2(b). The contribution from $\rho(1450)$ is larger than that from $\rho(770)$ - a somewhat unlikely result. As observed in the previous analysis¹⁰ of this channel with a similar model, the NR mode dominates.

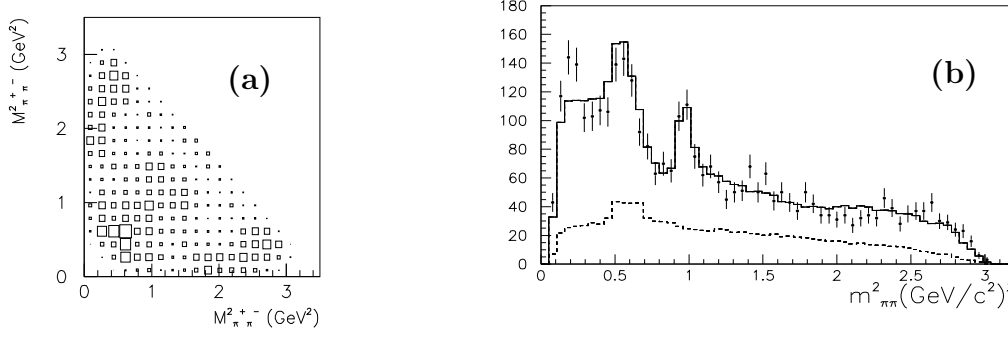


Figure 2: (a) Dalitz plot for $D^+ \rightarrow \pi^- \pi^+ \pi^+$ decays. (b) Projection of $\pi^- \pi^+$ effective mass. Data (points with errors) and predictions (solid line) from model III described in the text indicate poor agreement at low mass.

Adding a scalar amplitude (σ , similar to the κ in model II) results in a superior fit ($\chi^2/\nu = 0.9$). Results for this (model IV) are in table 1. Mass and width for σ are found to be $M_\sigma = 478^{+24}_{-23} \pm 17$ and $\Gamma_\sigma = 324^{+42}_{-40} \pm 21$ MeV/c². Both NR and $\rho(1450)\pi$ contributions are insignificant, and the $\sigma\pi$ amplitude is dominant. As for the κ , the s -wave BW form seems to be the best model of those applied to these data.

6 Conclusions.

We conclude that the s -wave $K^- \pi^+$ system from decay of D^+ to $K^- \pi^+ \pi^+$ has amplitude and phase variation consistent with a sum of NR, $K_0(1430)$ and scalar κ terms. Similarly, the s -wave $\pi^- \pi^+$ system from decay of $D^+ \rightarrow \pi^- \pi^+ \pi^+$ has amplitude and phase variation consistent with a sum of NR, $f_0(980)$ and scalar σ terms. Though this hints at the existence of scalar κ and σ resonances, use of Breit Wigner functions to describe such broad states near threshold may not be appropriate, and other interpretations of the data may be possible.

References

1. K. Hagiwara et al., *Phys. Rev. D* **66**, 010001 (2002).
2. E691 collaboration, J. C. Anjos et al., *Phys. Rev. D* **48**, 56 (1993).
3. E687 collaboration, P. L. Frabetti et al., *Phys. Lett. B* **331**, 217 (1994).
4. E791 collaboration, E. M. Aitala et al., *Phys. Rev. Lett.* **86**, 770 (2000).
5. E791 collaboration, E. M. Aitala et al., *accepted by Phys. Rev. Letters*, hep-ex/0204018.
6. E791 collaboration, E. M. Aitala et al., *Eur. Phys. J. direct* **C4**, 1 (1999).
7. S. Amato et al., *Nucl. Instrum. Methods* **A324**, 535 (1993); S. Bracker et al., hep-ex/9511009.
8. CLEO collaboration, S. Kopp et al., *Phys. Rev. D* **63**, 092001 (2001).
9. W. M. Dunwoodie (for LASS collaboration), *private communication*. A recent re-fit to $I = 1/2$ s -wave $K\pi$ elastic scattering data below $K\eta'$ threshold yields $M = 1435 \pm 5$, $\Gamma = 279 \pm 40$ MeV/c² compared to PDG values 1412 ± 6 and 294 ± 23 MeV/c² respectively.
10. E687 collaboration, P. L. Frabetti et al., *Phys. Lett. B* **407**, 79 (1997).